The metal-rich bulge globular cluster NGC 6401[*]

B. Barbuy[1], **S. Ortolani**[2,3], **E. Bica**[4], **and S. Desidera**[2]

[1] Universidade de São Paulo, CP 3386, São Paulo 01060-970, Brazil (barbuy@orion.iagusp.usp.br)
[2] Università di Padova, Dept. di Astronomia, Vicolo dell'Osservatorio 5, I-35122 Padova, Italy (ortolani, desidera@pd.astro.it)
[3] European Southern Observatory, Karl-Schwarzschild-Strasse 2, D-85748, Garching bei München, Germany (sortolan@eso.org)
[4] Universidade Federal do Rio Grande do Sul, Dept. de Astronomia, CP 15051, Porto Alegre 91501-970, Brazil (bica@if.ufrgs.br)

Abstract. We present V and I photometry for the bulge globular cluster NGC 6401 for the first time. The Colour-Magnitude Diagram reveals a red horizontal branch, and the cluster is metal-rich ([Fe/H] $\approx$ -0.7). NGC 6401 is located at 5.3° from the Galactic center, turning out to be an interesting target to trace the extent of the bulge.

A reddening E(B-V) = 0.53$\pm$0.15 and a distance from the Sun $d_\odot \approx$ 12.0$\pm$1.0 kpc are derived. The cluster is slightly behind the bulk of the bulge population in that direction, but still within the bulge volume.

Since the number of clusters with Horizontal Branch information has increased enormously in the later years for the central 20°$\times$20°, we present a discussion on the distribution of red and blue horizontal branch clusters and their possible relation to bulge and/or halo.

Key words: stars: Hertzsprung–Russel (HR) and C-M diagrams – Galaxy: globular clusters: individual: NGC 6401

1. Introduction

Recently we have completed a CCD Colour-Magnitude Diagram (CMD) survey of the known globular clusters within 5° of the Galactic center, deriving accurate parameters, and the results are gathered in Barbuy et al. (1998a), where we discuss the overall structure and other characteristics of the old population of the central regions of the Galaxy. In Barbuy et al. (1998a) the sample consisted of 16 clusters out of the 17 known clusters in the region; the missing object Terzan 9 is now studied (Ortolani et al. 1999b).

Our focus is now turned towards a wider region extending to a 20°$\times$20° box around the Galactic center. This region is fundamental since it contains the transition bulge-halo (e.g. Minniti 1995a).

CCD CMDs obtained for clusters in the ring 5° $<$ r $<$ 20° have been steadily increasing in the last years, such as: M80 (NGC 6093) (Brocato et al. 1998), NGC 6256, NGC 6717 (Palo-

mar 9) (Ortolani et al. 1999a; Brocato et al. 1996), NGC 6287 (Stetson & West 1995), NGC 6316, NGC 6342, NGC 6496, NGC 6539, Palomar 8 (Armandroff 1988), NGC 6380 and Terzan 12 (Ortolani et al. 1998), NGC 6558 (Rich et al. 1998), Terzan 3 and IC 1276 (Palomar 7) (Barbuy et al. 1998b) and Tonantzintla 2 (Bica et al. 1996). Not all clusters projected on the studied ring will be within the bulge volume, such as the case of IC 1257 for which Harris et al. (1997) derived a distance of 24 kpc from the Sun, thus placing it in the halo on the other side of the Galaxy.

NGC 6401 is a globular cluster projected in the studied region, and its parameters are not well determined in the literature. In particular, no optical CMDs are available. Minniti et al. (1995) presented an infrared CMD for this cluster, detecting the red giant branch (RGB), but not clearly reaching the horizontal branch (HB) level.

NGC 6401, also named ESO520-SC11 and GCL1735-238, is located at α_{2000} = 17^h 38^m 36.9^s, δ_{2000} = -23° 54′ 32″ (l = 3.45°, b = 3.98°). Zinn & West (1984) report [Fe/H] = -1.13 derived from integrated spectroscopy. Bica & Alloin (1986), by means of a visible integrated spectrum, have found that line strengths and continuum distributions are compatible with [Fe/H] = -1.1 and E(B-V) = 0.81. Hesser & Shawl (1985) report an integrated spectral type F9, suggesting that the cluster could be moderately metal-rich. Webbink (1985) and Harris (1996) compilations provide respectively the following parameters: [Fe/H] = -1.01 and -1.12, V_{HB} = 17.3 and 17.7, E(B-V) = 0.76 and 0.85, $d_\odot$ = 7.1 and 7.2 kpc. Minniti (1995b) derived [Fe/H] = -1.10 and E(B-V) = 0.59. NGC 6401 shows some concentration with c = 1.69 (Trager et al. 1995).

In Sect. 2 the observations are described. In Sect. 3 we discuss the Colour-Magnitude Diagram and determine cluster parameters. In Sect. 4 a discussion of bulge or halo membership is given in the frame of a cluster sample in the central parts of the Galaxy.

2. Observations

NGC 6401 was observed in the night of July 4, 1998, with the 1.5m Danish telescope at ESO (La Silla). We employed an EFOSC camera equipped with a Loral/Lesser CCD detector C1W7 with 2052$\times$2052 pixels. The pixel size is 15 μm, cor-
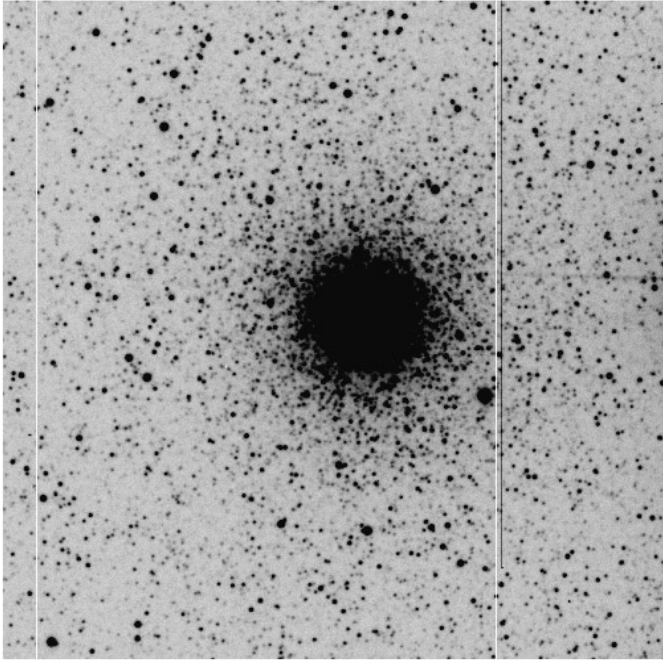

Fig. 1. V image (15 sec.) of NGC 6401. Dimensions are $6.5' \times 6.5'$. North at the top and east to the left.

responding to $0.39''$ on the sky, which provides a full field of $13' \times 13'$.

In Fig. 1 we show a 15 sec V exposure of NGC 6401, where it is clear that we are dealing with a rich cluster.

In the same night the template cluster 47 Tucanae was also observed, in order to have its bright sequences compared to those of NGC 6401. The frame is offset by $5'$ south relative to the cluster center. This template V vs. (V-I) CMD diagram is shown in Fig. 2.

The log of observations is provided in Table 1.

Daophot II was used to extract the instrumental magnitudes. For calibrations we used stars from Landolt (1983) and Landolt (1992).

Reduction procedures in such reddened crowded fields were discussed in detail in a study of Liller 1 (Ortolani et al. 1996 and references therein). The equations for the present clusters are:

$$V = 24.26 + v$$
$$I = 23.10 + i$$

reduced to 1 sec. exposure time and 1.1 airmass. Due to crowding effects arising in the transfer of the aperture magnitudes from standards to the field stars, the zero point calibration errors are dominant, estimated to be about ± 0.03 mag. The CCD shutter time uncertainty (0.3 sec) for a typical 10s exposure time for the standard stars, produces an additional 3% uncertainty, which is propagated to the calibrations of the long exposure cluster frames. The final magnitude zero point uncertainty amounts to ± 0.05. The atmospheric extinction was corrected with the La Silla coefficients ($C_V = 0.16$, $C_I = 0.12$ mag/airmass).
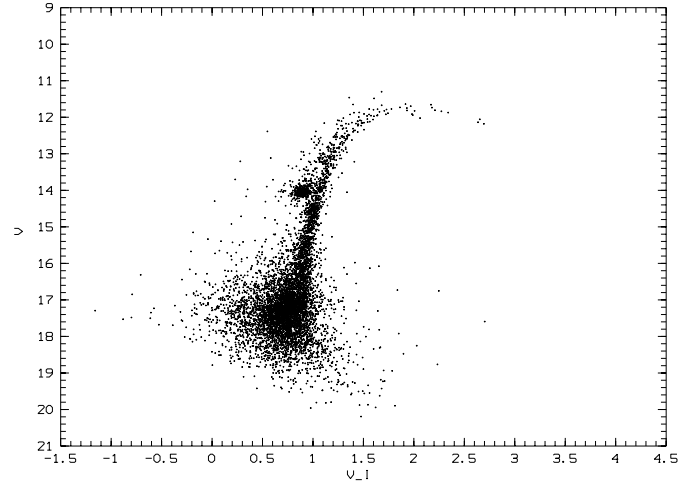

Fig. 2. V vs (V-I) CMD of the template 47 Tucanae, observed in the same night as NGC 6401. The sampling corresponds to an extraction of 1000 x 1000 pixels ($6.5' \times 6.5'$).
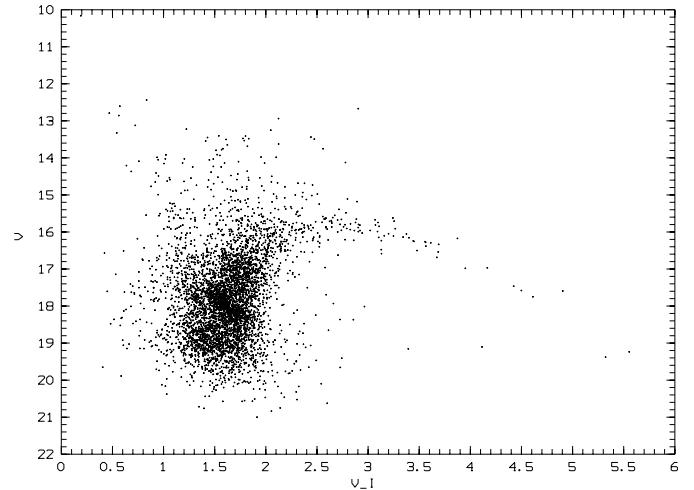

Fig. 3. V vs. (V-I) CMD for an extraction 1000×1000 pixels ($6.5' \times 6.5'$) centered on NGC 6401.

3. NGC 6401

3.1. Colour-magnitude diagrams

In Fig. 3 we show the V vs. (V-I) diagram of NGC 6401 in an extraction of 1000×1000 pixels ($6.5' \times 6.5'$). We see two red horizontal branches (RHB), a prominent one at $V \approx 18$ and a more diffuse and less populated one at $V \approx 17$. In the following it will become clear that the fainter RHB belongs to the cluster, while the brighter one belongs to the bulge field. We also see a curved and extended red giant branch (RGB) reaching (V-I) ≈ 5.5, characteristic of metal-rich populations (Barbuy et al. 1998a).

In Fig. 4a we show a V vs. (V-I) CMD corresponding to a circular extraction of 400 pixels (r < 2.6') centered on the cluster, excluding the central 20 pixels (r < 8'') to avoid overcrowding. In this figure the cluster features are enhanced: in particular, the cluster RHB becomes more prominent with respect to that of
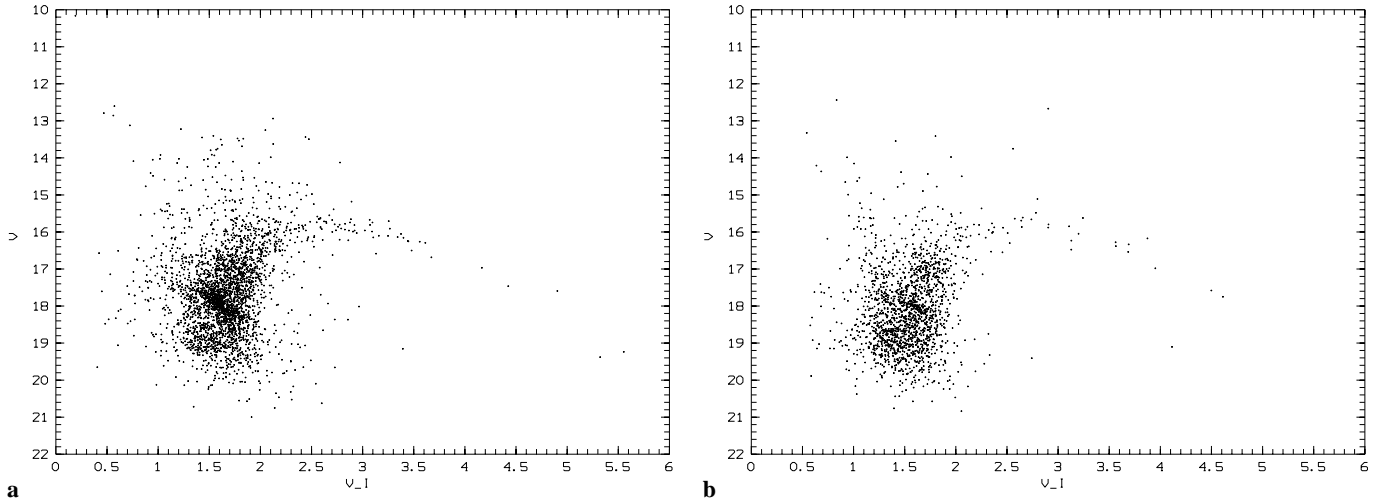
Fig. 4a and b. V vs. (V-I) CMDs for: **a** circular extraction of 400 pixels (r < 2.6′) centered on the cluster, excluding the central 20 pixels (r < 8″) **b** extraction of r > 2.6′, showing field sequences.

Table 1. Log of observations

Target	Filter	Exp. (sec.)	Seeing (″)
NGC 6401	V	15	1.6
	I	10	1.6
47 Tuc	V	8	2.0
	I	4	2.0

the field, as compared to Fig. 3. In Fig. 4b we avoid the cluster main area, by showing a CMD corresponding to an extraction of r > 2.6′, where the field sequences are expected to be enhanced. In fact, the cluster RHB (V ≈ 18.0) is minimized as compared to that of Fig. 4a. The field RHB (V ≈ 17.0) on the other hand is enhanced. In Fig. 4b the field blue main sequence (MS) also becomes clear.

In Fig. 5 we show an offset field located 7′ north-east of the cluster. The size of this extracted field is 700×700 pixels (4.6′×4.6′). The bulge field sequences already seen in Fig. 4b are confirmed. Overimposed on Fig. 5 is the mean locus of the metal-rich globular cluster NGC 6553 (Z ≈ Z$_\odot$, Barbuy et al. 1999), which is also a template for the Baade Window (Ortolani et al. 1995b). The field HB and corresponding RGB are comparable to that of the Baade Window, which is not unexpected given the present field latitude (b = 4°). Notice that the HB is located at V ≈ 17.3, slightly fainter and also redder than the field HB level of Fig. 4b, caused by a difference in reddening.

In Fig. 6 we give an optimal cluster extraction of 200 < r < 300 pixels or 1.3′ < r < 2.0′, to constrain the cluster metallicity. A best description is obtained by the mean locus of 47 Tuc ([Fe/H] = -0.7, Zinn & West 1984), as seen by its mean locus superposed to the cluster sequences in Fig. 6.

It is remarkable, as seen in Figs. 4, and corroborated from the fits of Figs. 5 and 6, that the location of the RGB cool extended sequence in the closer bulge field (more metal-rich), overlaps

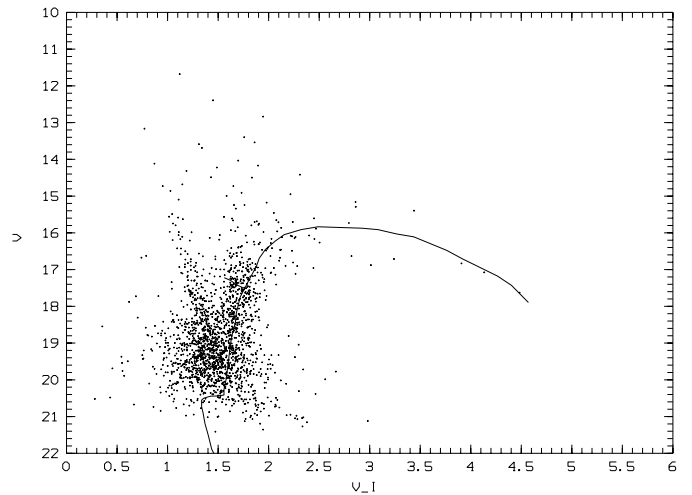**Fig. 5.** V vs. (V-I) CMD of offset field (7′ NE of cluster). Mean locus of NGC 6553 is overimposed.
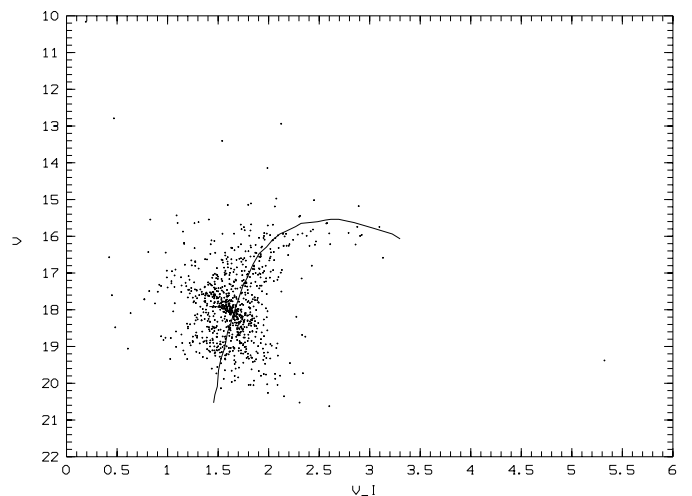

Fig. 6. NGC 6401: V vs. (V-I) optimal cluster extraction of 200 < r < 300 pixels (1.3′ < r < 2.0′). Overimposed is the mean locus of 47 Tuc.
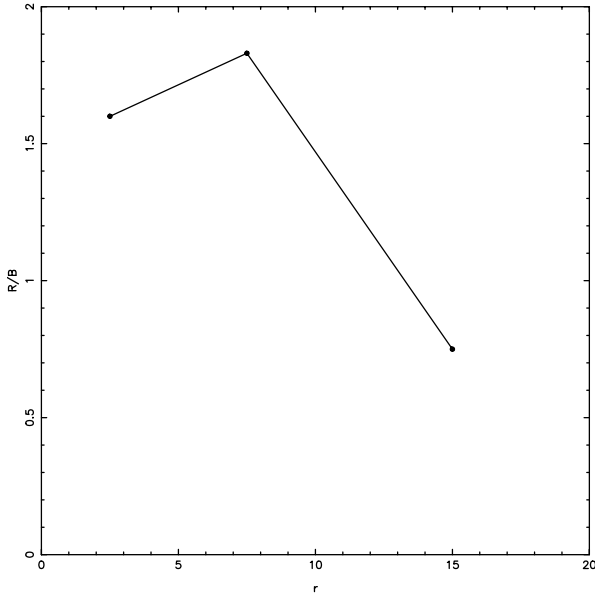
Fig. 7. Ratio of R/B clusters as a function of radius r = $\sqrt{l^2 + b^2}$ for the bins 0 °< r < 5°, 5° < r < 10° and 10 °< r < 20°.
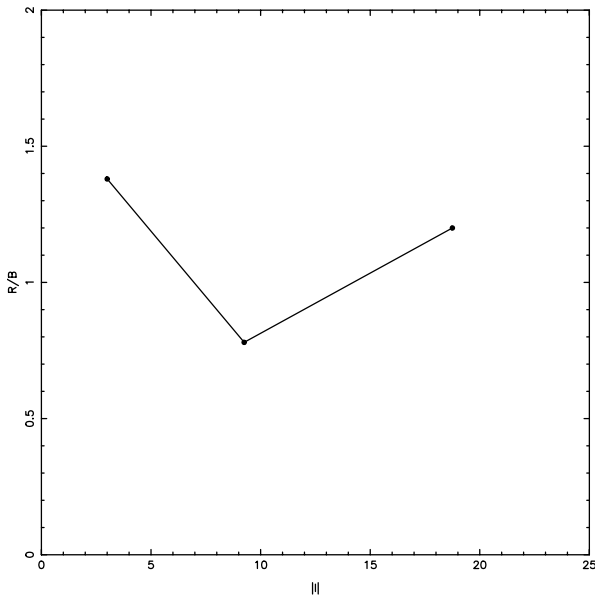
Fig. 8. R/B is plotted as a function of longitude with bins 0 °< |l| < 6°, 6 °< |l| < 12.5° and 12.5 °< |l| < 25°.

that of the more distant RGB of NGC 6401 (which appears to be 47 Tuc-like in metallicity).

3.2. Cluster reddening and distance

The cluster HB is located at V = 18.0±0.15 and the (V-I) colour of the RGB at the HB level is (V-I) = 1.70±0.08. The reddening is derived with respect to 47 Tuc from the overall fit on the optimal extraction of Fig. 6. We derive Δ(V-I)(NGC6401-47Tuc) = 0.65 and E(V-I) = 0.70 adopting E(V-I)$_{47\text{Tuc}}$ = 0.05 (Barbuy et al. 1998a and references therein). Adopting E(V-I)/E(B-V) =

1.31 (Dean et al. 1978), we obtain E(B-V) = 0.53±0.15, and adopting R = 3.25 (Barbuy et al. 1998a and references therein), suitable for this metallicity, we get A$_V$ = 1.74.

An absolute magnitude of the horizontal branch M$_V^{HB}$ = 0.85 (Buonanno et al. 1989) is adopted for the cluster metallicity. The resulting absolute distance modulus is (m-M)$_\circ$ = 15.4, and the distance to the Sun d$_\odot$ = 12.0±1.0 kpc. (Note that if the ratio E(V-I)/E(B-V) = 1.6 following Rieke & Lebofsky (1985) is adopted, we obtain instead A$_V$ = 1.42, and the cluster will be found consequently more distant by 2 kpc; this uncertainty is not included in the error bar for the distance). We assume the distance of the Sun to the Galaxy center to be R$_\odot$ = 8.0 kpc (Reid 1993), in order to be consistent with Barbuy et al. (1998a), but we point out that in more recent work by Reid (1998) higher values are given; the Galactocentric coordinates are then X = 3.95 (X<0 refers to our side of the Galaxy), Y = 0.72 kpc and Z = 0.83 kpc. The distance from the Galactic center is R$_{GC}$ = 4.1 kpc. Therefore the cluster is behind the bulk of the bulge population (Sect. 3.3).

3.3. Parameters for the field

The fit of the offset field (Fig. 5) gives an HB level at V ≈ 17.3±0.2 and the (V-I) colour of the RGB at the HB level is (V-I) = 1.75±0.15. The reddening is derived with respect to NGC 6553 resulting Δ(V-I)(NGC6553-field) = 0.35 and E(V-I) = 0.60 adopting E(V-I)$_{NGC6553}$ = 0.95 (Guarnieri et al. 1998). Assuming E(V-I)/E(B-V) = 1.31 (Dean et al. 1978), we obtain E(B-V) = 0.46, and with R = 3.47 (Barbuy et al. 1998a and references therein), suitable for this metallicity, we get A$_V$ = 1.59.

An absolute magnitude of the horizontal branch M$_V^{HB}$ = 0.95 is adopted for the cluster metallicity. The resulting absolute distance modulus is (m-M)$_\circ$ = 14.76, and the distance to the Sun d$_\odot$ = 8.9±1.0 kpc.

We conclude that the bulk field population in this direction is foreground to the cluster.

4. Discussion and concluding remarks

NGC 6401 adds now to a list of about 70 clusters within a box of 20°×20° around the Galactic center, for which reliable information on the HB morphology, reddening and distances are available.

In order to understand the families of globular clusters in the central parts of the Galaxy, and how they correlate with the bulge and the bulge-halo transition region, we gathered in Table 2 clusters with CMDs deep enough to allow a classification in terms of HB morphology.

The clusters projected in the selected region which are however located at distances larger than R$_{GC}$ > 4.5 kpc were eliminated, since they probably do not belong to the bulge volume. By bulge volume we mean a large enough distance trying to allow inclusion of bulge clusters in apogalacticon.

We also have not considered the clusters of the Sagittarius dwarf galaxy projected in the present region: Arp 2, Terzan 7

Table 2. Clusters projected on the bulge for which HB morphology is determined

Target	l	b	HB type	ref.
Djorgovski 1	356.68	-2.48	R	1
ESO452-SC11	351.91	12.10	I	2
ESO456-SC38	2.76	-2.51	R	3
HP 1	357.43	2.12	B	4
IC 1276	21.83	5.67	R	5
Liller 1	354.84	-0.16	R	6
M9 (NGC 6333)	5.54	10.71	B	7
M14 (NGC 6402)	21.32	14.81	B	8
M19 (NGC 6273)	356.87	9.38	B	9
M28 (NGC 6626)	7.80	-5.58	B	10
M62 (NGC 6266)	353.58	7.38	B	11
M69 (NGC 6637)	1.72	-10.27	R	12
M70 (NGC 6681)	2.85	-12.51	B	13
M80 (NGC 6093)	352.67	19.46	B	14
NGC 5986	337.02	13.27	B	15
NGC 6139	342.37	6.94	B	16,17
NGC 6144	351.93	15.70	B	18
NGC 6235	358.92	13.52	B	19
NGC 6256	347.79	3.31	B	20
NGC 6287	0.13	11.02	B	21
NGC 6293	357.62	7.83	B	7
NGC 6304	355.83	5.38	R	22
NGC 6316	357.18	5.76	R	23
NGC 6342	4.90	9.73	R	23
NGC 6352	341.42	-7.17	R	24
NGC 6356	6.72	10.22	R	25
NGC 6380	350.18	-3.42	R	26
NGC 6388	345.56	-6.74	R/BT*	27
NGC 6401	3.45	3.98	R	present
NGC 6440	7.77	3.80	R	28
NGC 6441	353.53	-5.01	R/BT*	27
NGC 6453	355.72	-3.87	B	16
NGC 6496	348.03	-10.01	R	23
NGC 6517	19.23	6.76	B	29
NGC 6522	1.03	-3.93	B	30,31,32
NGC 6528	1.14	-4.17	R	33
NGC 6539	20.80	6.78	R	23
NGC 6541	349.29	-11.18	B	34
NGC 6553	5.25	-3.02	R	33
NGC 6558	0.20	-6.03	B	35
NGC 6624	2.79	-7.91	R	36
NGC 6638	7.90	-7.15	I	37
NGC 6652	1.53	-11.38	R	38
NGC 6717 (Pal 9)	12.88	-10.90	B	20,13
NGC 6723	0.07	-17.30	I/BT*	39
Palomar 6	2.09	1.78	R	1
Palomar 8	14.11	-6.80	R	23
Terzan 1	357.57	1.00	R	40
Terzan 2	356.32	2.30	R	41
Terzan 3	345.08	9.19	R	5
Terzan 4	356.02	1.31	B	42
Terzan 5	3.81	1.67	R	43
Terzan 6	358.57	-2.16	R	44
Terzan 9	3.60	-1.99	B	16
Terzan 10	4.42	-1.86	B	3

Table 2. (continued)

Target	l	b	HB type	ref.
Terzan 12	8.36	-2.10	R	26
Tonantzintla 2	350.8	-3.42	R	45
UKS 1	5.13	0.76	R	3,6

* BT = Blue Tail; *References:* 1 Ortolani et al. (1995a); 2 Bica et al. (1999); 3 Ortolani et al. (1997a); 4 Ortolani et al. (1997b); 5 Barbuy et al. (1998b); 6 Ortolani et al. (1999c); 7 Janes & Heasley (1991); 8 Shara et al. (1986); 9 Harris et al. (1976); 10 Rees & Cudworth (1991); 11 Brocato et al. (1996); 12 Ferraro et al. (1994); 13 Brocato et al. (1996); 14 Brocato et al. (1998); 15 Harris (1996); 16 Ortolani et al. (1999b); 17 Zinn & Barnes (1998); 18 Alcaino (1980); 19 Liller (1980); 20 Ortolani et al. (1999a); 21 Stetson & West (1995); 22 Davidge et al. (1992); 23 Armandroff (1988); 24 Fullton et al. (1995); 25 Bica et al. (1994); 26 Ortolani et al. (1998); 27 Rich et al. (1997); 28 Ortolani et al. (1994a); 29 Kavelaars et al. (1995); 30 Terndrup & Walker (1994); 31 Barbuy et al. (1994); 32 Shara et al. (1998); 33 Ortolani et al. (1995b); 34 Alcaino (1979); 35 Rich et al. (1998); 36 Sarajedini & Norris (1994); 37 Alcaino & Liller (1983); 38 Ortolani et al. (1994b); 39 Fullton & Carney (1994); 40 Ortolani et al. (1999d); 41 Ortolani et al. (1997c); 42 Ortolani et al. (1997d); 43 Ortolani et al. (1996); 44 Barbuy et al. (1997); 45 Bica et al. (1996).

and M54 (NGC 6715), and clusters projected on the region but clearly not related to the bulge volume: IC 1257, NGC 6540, M4 (NGC 6121), NGC 6284, M22 (NGC 6656), NGC 6366, NGC 6544 and NGC 6584.

The basic sources for distances and HB morphology are Harris (1996) compilation and Barbuy et al. (1998a), and new data in the recent literature.

In Table 2 the clusters are classified as R, B or I, which means horizontal branches R: very red, B: very blue or I: with intermediate characteristics. We find a total of 58 clusters which fit the selection criteria, of which 31 are R, 27 are B or I. We point out that in the cases of Blue Tails of NGC 6388 and NGC 6441 (Rich et al. 1997) the clusters are in the R group, since their red HBs are very populated.

The number of metal-rich (R) clusters is comparable to that of metal-poor (B or I) ones. This is not unexpected since Minniti (1995a) predicted a large fraction of halo clusters in the bulge volume. Besides, metal-poor bulge clusters are likely to exist, meaning that they formed in the bulge at early times maintaining orbits characteristic of the bulge.

In Fig. 7 we plot the ratio of R/(B+I) clusters as a function of radius $r = \sqrt{l^2 + b^2}$ for the bins $0° < r < 5°$, $5° < r < 10°$ and $10° < r < 20°$. The ratio R/B decreases steadily from the center to increasing distances. This behaviour is expected in a scenario of interloping bulge and halo (Minniti 1995a); note that the observed sample is not complete given that (i) we considered only clusters with the complete information, (ii) in the extremely reddened parts of the bulge it is probable that a number of clusters remain undetected.

In Fig. 8 the same ratio R/(B+I) is plotted as a function of longitude with bins $0° < |l| < 6°$, $6° < |l| < 12.5°$ and $12.5° < |l| < 25°$. This longitude dependence of the ratio R/B shows

a minimum around 9°. The drop is expected in a bulge/halo spheroidal scenario, and the increase for larger longitudes could be due to a globular cluster population related to the thick disk, which is also expected (see e.g. Armandroff 1989 and the three component model of Minniti 1995a).

We conclude that NGC 6401 is a bulge metal-rich cluster which is part of a crucial sample in the Galaxy, that might be the key to understand the bulge/halo transition region. Spectroscopic observations of individual giants in view of abundance and kinematical studies would help constrain such models.

References

Alcaino G., 1979, ApJS 35, 233

Alcaino G., 1980, A&AS 39, 315

Alcaino G., Liller W., 1983, AJ 88, 1166

Armandroff T.E., 1988, AJ 96, 588

Armandroff T.E., 1989, AJ 97, 375

Aurière M., Ortolani S., 1988, A&A 204, 105

Barbuy B., Ortolani S., Bica E., 1994, A&A 285, 871

Barbuy B., Ortolani S., Bica E., 1997, A&AS 122, 483

Barbuy B., Bica E., Ortolani S., 1998a, A&A 333, 117

Barbuy B., Ortolani S., Bica E., 1998b, A&AS 132, 333

Barbuy B., Renzini A., Ortolani S., Bica E., Guarnieri M.D., 1999, A&A 341, 539

Bica E., Allain D., 1986, A&AS 66, 171

Bica E., Ortolani S., Barbuy B., 1994, A&AS 106, 161

Bica E., Ortolani S., Barbuy B., 1996, A&AS 120, 153

Bica E., Ortolani S., Barbuy B., 1999, A&AS 136, 363

Brocato E., Buonanno R., Malakhova Y., Piersimoni A.M., 1996, A&A 311, 778

Brocato E., Castellani V., Scotti G.A., et al., 1998, A&A 335, 929

Buonanno R., Corsi C.E., Fusi Pecci F., 1989, A&A 216, 80

Chaboyer B., Demarque P., Sarajedini A., 1996, ApJ 459, 558

Davidge T.J., Harris W.E., Bridges T.J., Hanes D.A., 1992, ApJS 81, 251

Dean J.F., Warren P.R., Cousins A.W.J., 1978, MNRAS 183, 569

Desidera S., Ortolani S., 1997, In: Bedding T., Booth A., Davis J. (eds.) IAU Symp. 189, Fundamental stellar parameters: the interaction between observations and theory. Poster papers, p. 164

Ferraro F.R., Fusi-Peci F., Guarnieri M.D., et al., 1994, MNRAS 266, 829

Fullton L.K., Carney B.W., 1994, BAAS 186, 9703

Fullton L.K., Carney B.W., Olszewski E.W., et al., 1995, AJ 119, 652

Gratton R.G., Ortolani S., 1988, A&AS 73, 137

Guarnieri M.D., Ortolani S., Montegriffo P., 1998, A&A 331, 70

Harris W.E., Racine R., de Roux J., 1976, ApJS 31, 13

Harris W.E., 1996, AJ 112, 1487

Harris W.E., Phelps R.L., Madore B.F., et al., 1997, AJ 113, 688

Hesser J.E., Shawl S.J., 1985, PASP 97, 465

Hesser J.E., Harris W.E., Vandenberg D.A., Allwright J.W.B., 1987, PASP 99, 7 39

Holtzman J.A., Light R.M., Baum W.A., et al., 1993, AJ 106, 1826

Iben I. Jr., 1974, ARA&A 12, 215

Janes K.A., Heasley J.N., 1991, AJ 101, 2097

Jones R.V., Carney B.W., Storm J., Latham D.W., 1992, ApJ 386, 646

Kavelaars J.J., Hanes D.A., Bridges T.J., Harris W.E., 1995, AJ 109, 2081

Kinman T.D., Rosino L., 1962, PASP 74, 499

Kiraga M., Paczynski B., Stanek K.Z., 1997, ApJ 485, 616

Landolt A.U., 1983, AJ 88, 439

Landolt A.U., 1992, AJ 104, 340

Liller M.H., 1980, AJ 85, 673

Minniti D., 1995a, AJ 109, 1663

Minniti D., 1995b, A&A 303, 468

Minniti D., Olzewski E.W., Rieke M., 1995, AJ 110, 1686

Ortolani S., Barbuy B., Bica E., 1990, A&A 236, 362

Ortolani S., Barbuy B., Bica E., 1994a, A&AS 108, 653

Ortolani S., Barbuy B., Bica E., 1994b, A&A 286, 444

Ortolani S., Barbuy B., Bica E., 1996, A&A 308, 733

Ortolani S., Bica E., Barbuy B., 1995a, A&A 296, 680

Ortolani S., Renzini A., Gilmozzi R., et al., 1995b, Nat 377, 701

Ortolani S. Bica E., Barbuy B., 1997a, A&AS 126, 319

Ortolani S., Bica E., Barbuy B., 1997b, MNRAS 284, 692

Ortolani S., Bica E., Barbuy B., 1997c, A&A 326, 614

Ortolani S., Barbuy B., Bica E., 1997d, A&A 319, 850

Ortolani S., Bica E., Barbuy B., 1998, A&AS 127, 471

Ortolani S., Barbuy B., Bica E., 1999a, A&AS 136, 237

Ortolani S., Bica E., Barbuy B., 1999b, A&A, in press

Ortolani S., Bica E., Barbuy B., et al., 1999c, in preparation

Ortolani S., Bica E., Barbuy B., et al., 1999d, A&A submitted

Rees R.F., Cudworth K.M., 1991, AJ 102, 152

Reid M., 1993, ARA&A 31, 345

Reid M., 1998, AJ 115, 205

Rich R.M., Sosin R.M., Djorgovski S.G., et al., 1997, ApJ 484, L25

Rich R.M., Ortolani S., Bica E., Barbuy B., 1998, AJ 116, 1295

Rieke G.H., Lebofsky M.J., 1985, ApJ 288, 618

Sandage A., 1986, ARA&A 24, 421

Sarajedini A., Norris J.E., 1994, ApJS 93, 161

Shara M.M., Moffat A.F., Potter M., Hogg H.S., Wehlau A., 1986, ApJ 311, 796

Shara M.M., Drissen L., Rich R.M., et al., 1998, ApJ 495, 796

Stetson P.B., West M.J., 1995, PASP 106, 726

Terndrup D.M., Walker A.R., 1994, AJ 107, 1786

Terzan A., 1968, Comptes Rendus Acad. Sci. 267, 1245

Trager S.C., King I.R., Djorgovski S., 1995, AJ 109, 218

Webbink R.F., 1985, In: Goodman J., Hut P. (eds.) Dynamics of Star Clusters. IAU Symp. 113, Reidel, Dordrecht, 541

Zinn R., 1985, ApJ 293, 424

Zinn R., Barnes S., 1998, AJ 116, 1736

Zinn R., West M.J., 1984, ApJS 55, 45